Roscovitine Modulates DNA Repair and Senescence: Implications for Combination Chemotherapy

Elvira Crescenzi,[1] Giuseppe Palumbo,[1] and Hugh J.M. Brady[2]

Abstract

Purpose: Treatment of tumor cells by chemotherapy activates a series of responses ranging from apoptosis to premature senescence and repair. Survival responses are characterized by inhibition of cyclin-dependent kinases. Because inhibition of cyclin-dependent kinases represents a distinctive feature of DNA damage – induced prosurvival responses, we investigated the possibility that the cyclin-dependent kinase inhibitor roscovitine modulates drug-induced responses in human adenocarcinoma cells, favoring cell survival.

Experimental Design: Sublethal concentrations of doxorubicin were used to induce premature senescence in human adenocarcinoma cells. The effect of the cyclin-dependent kinase inhibitor roscovitine on the doxorubicin-dependent cell cycle checkpoint activation and DNA repair pathways was evaluated.

Results: Roscovitine reinforces doxorubicin-dependent G_1 checkpoint in A549 and HEC1B cells leading to decreased frequency of double-strand breaks and to the preferential induction of senescence and enhanced clonogenic survival. However, in other tumor cell lines, such as HCT116 and H1299, combined treatment with doxorubicin and roscovitine increases the frequency of double-strand breaks and dramatically sensitizes to doxorubicin. This unexpected effect of roscovitine depends on a novel ability to inhibit DNA double-strand break repair processes and requires inactivation of the pRb pathway.

Conclusions: Roscovitine, by hindering DNA repair processes, has the potential to inhibit recovery of mildly damaged tumor cells after doxorubicin treatment and to increase the susceptibility of tumor cells to chemotherapy. However, in some tumor cells, the cell cycle inhibitory function of roscovitine prevails over the DNA repair inhibitory activity, favoring premature senescence and clonogenic growth. These data indicate a novel mechanism underlying combined chemotherapy, which may have wide application in treatment of carcinomas.

Chemotherapy is the primary form of treatment for human cancer. Conventional anticancer drugs damage several cellular components, triggering a series of cellular responses. At high doses of these drugs, the predominant effect is cell death, whereas at low doses tumor cells may repair damage and eventually resume normal proliferation (1). Cell death after DNA damage is largely the result of apoptosis, and accordingly, apoptosis is a key determinant of treatment outcome (2). However, although apoptosis represents the main response to chemotherapy in hematologic malignancies, the outcome of therapy in solid tumors does not correlate with the extent of programmed cell death (3). In solid tumors, treatment does not lead to tumor regression but rather results in so-called stable disease. The cytostatic effect of chemotherapeutic agents results from the activation of a premature senescence program (1). Accordingly, treatment of tumor cell lines with low doses of DNA-damaging agents readily induces features of senescence (4). More importantly, the induction of a senescent-like phenotype by anticancer drugs can be induced *in vivo* and contributes to successful treatment (5).

Factors that modulate stress-induced premature senescence have not yet been extensively studied. Stress-induced senescent cells acquire a distinctive morphology and the expression of specific phenotypic markers, such as acidic senescence-associated β-galactosidase (SA-β-gal). In addition, a distinctive feature of senescent cells is the increased expression of cyclin-dependent kinase (Cdk) inhibitors, which seems to be responsible for the permanent cytostatic arrest. Inhibition of Cdk activity also represents a key feature of DNA damage checkpoints (6).

Roscovitine is a small molecule that inhibits Cdks via direct competition in the ATP-binding site. It is particularly active against Cdk1 (Cdc2), Cdk2, and Cdk5 (7) and induces G_1 and G_2-M arrest in cells. High doses of roscovitine induce apoptosis in tumor cells (8, 9). Because inhibition of Cdk activity

Authors' Affiliations: [1]Dipartimento di Biologia e Patologia Cellulare e Molecolare "L. Califano" and Centro di Endocrinologia ed Oncologia Sperimentale-Consiglio Nazionale delle Ricerche Facoltà di Medicina e Chirurgia, Università di Napoli "Federico II," Naples, Italy and [2]Molecular Haematology and Cancer Biology Unit, Institute of Child Health, University College of London, London, United Kingdom

Received 5/16/05; revised 8/11/05; accepted 8/22/05.

Grant support: Ministero dell'Istruzione, dell'Università e della Ricerca-COFIN 2002 Program and Agenzia Spaziale Italiana (G. Palumbo), Medical Research Council UK grant G9900172, and Olivia Hodson Fellowship Fund (H.J.M. Brady).

The costs of publication of this article were defrayed in part by the payment of page charges. This article must therefore be hereby marked advertisement in accordance with 18 U.S.C. Section 1734 solely to indicate this fact.

Requests for reprints: Hugh J.M. Brady, Molecular Haematology and Cancer Biology Unit, Institute of Child Health, University College London, 30 Guilford Street, London WC1N 1EH, United Kingdom. Phone: 44-20-79052731; Fax: 44-20-78138100; E-mail: h.brady@ich.ucl.ac.uk.

doi:10.1158/1078-0432.CCR-05-1042

represents a common feature of DNA damage–induced prosurvival responses, we decided to investigate the possibility that roscovitine modulates drug-induced damage responses in human adenocarcinoma cells, favoring the activation of senescence.

We show that roscovitine reinforces the G_1 checkpoint in doxorubicin-treated A549 and HEC1B cells. Augmentation of G_1 arrest reduces the extent of DNA damage and results in the preferential induction of a senescence program and in a chemoprotective effect of roscovitine. However, in several other human adenocarcinoma cells studied, roscovitine treatment dramatically sensitizes cells to doxorubicin-induced DNA damage. The ability of roscovitine to greatly sensitize certain tumor cells to DNA damage seems to require an inactive pRb pathway. These data indicate a novel mechanism underlying combined chemotherapy, which may have wide application in treatment of carcinomas.

Materials and Methods

Cell cultures and drug treatment. A549, HEC1B, HCT116, SW480, and H1299 cell lines were obtained from American Type Culture Collection (Rockville, MD) and cultured according to its instructions. MCF-7 and HeLa cells were cultured in DMEM, and MDA-MB-231 cells were cultured in RPMI. All media were supplemented with 10% FCS. Cell culture media and reagents were purchased by Invitrogen (San Giuliano Milanese, Milan, Italy). Doxorubicin (Calbiochem, San Diego, CA) was dissolved in sterile water (5 mg/mL stock solution). Roscovitine (Calbiochem) was dissolved in DMSO (5 mg/mL stock solution).

Growth assay and colony-forming efficiency. Cells were plated in triplicate at 2×10^4 per well in a 24-well plate. After 16 hours, cells were treated with roscovitine (10 μmol/L) or DMSO (vehicle). Cell number was assessed using a hemocytometer. Trypan blue (0.08%; Sigma, Milan, Italy) was added to evaluate cell viability. For colony-forming assay, cells were plated in triplicate at 5×10^4 in 60-mm dishes. After 8 to 10 days, colonies were stained with 1% methylene blue in 50% ethanol.

Senescence-associated β-galactosidase activity. Staining for SA-β-gal was done as described previously (10). Routinely, cells were plated in triplicate at 5×10^4 in 35-mm dishes or at 1×10^5 in 60-mm dishes.

Immunofluorescence microscopy. Cells were grown onto glass coverslips in six-well multidishes and allowed to adhere for 16 hours. Cells were fixed with methanol (−20°C) and permeabilized with ice-cold acetone. Cells were blocked with 10% fetal bovine serum in TBS-0.1% Tween 20 for 15 minutes. Phosphorylated histone H2AX (γ-H2AX) was detected by incubating the cells with anti-γ-H2AX monoclonal antibody in a 1:200 dilution for 2 hours. Cells were washed with TBS-0.1% Tween 20 and then incubated with 1:500 dilution of fluorescein-tagged goat anti-mouse secondary antibody (Santa Cruz Biotechnology, Santa Cruz, CA). After washes with TBS-0.1% Tween 20, the coverslips were mounted on a microscope slide using a 90% solution of glycerol in TBS and analyzed with a Zeiss Axioplan microscope. γ-H2AX foci were counted visually in >100 cells by capturing images of randomly chosen fields. Cells with >20 foci were excluded from quantitative analyses.

Flow cytometry for γ-H2AX. Cells were fixed with ethanol and routinely kept at −20°C overnight. Cells were washed twice with TBS and permeabilized with TBS, 4% fetal bovine serum, 0.1% Triton X-100 for 10 minutes on ice. Cells were washed with TBS and incubated with anti-γ-H2AX monoclonal antibody in a 1:200 dilution in TBS, 4% fetal bovine serum, for 2 hours. Cells were washed twice with TBS-0.1% Tween 20 and incubated with 1:200 dilution of fluorescein-tagged goat anti-mouse secondary antibody. After washes with TBS-0.1% Tween 20, cells were resuspended in TBS and analyzed using a FACScan cell scanner (Becton Dickinson, Franklin Lakes, NJ). Data were analyzed by the CellQuest software (BD Biosciences, Franklin Lakes, NJ).

Western blot analysis. Total cell proteins preparations were obtained lysing cells by 1 mmol/L EDTA, 0.2% Triton X-100, 1 μg/mL aprotinin, 170 μg/mL phenylmethylsulfonyl fluoride, and phosphatase inhibitors (Sigma). Protein concentration was routinely measured by the Bio-Rad protein assay (Milan, Italy). Polyacrylamide gels (7.5-15%) were prepared essentially as described by Laemmli (11). Molecular weight standards were from New England Biolabs (Hitchin, Herts, United Kingdom). Proteins separated on the polyacrylamide gels were blotted onto nitrocellulose filters (Hybond-C, Amersham, Bucks, United Kingdom). Filters were washed and stained with specific primary antibodies and then with secondary antisera conjugated with horseradish peroxidase diluted (1:2,000; Bio-Rad). Filters were developed using the enhanced chemiluminescence Western blotting detection reagent (Amersham) and quantitatively estimated by scanning with a Discover Pharmacia scanner equipped with a Sun Spark Classic Workstation. The anti-Bcl-2 (100), Bcl-X (S-18), Mcl-1 (S-19), Bax (N-20), $p27^{KIP1}$ (C-19), $p21^{CIP1}$ (C-19), cyclin E (M20), cyclin A (C-19), Cdk2 (M2), Cdk1 (17), $p16^{INK4a}$ (C-20), and p53 (DO-1) antibodies were purchased from Santa Cruz Biotechnology; anti-pRb (554136) was from BD Pharmingen (Franklin Lakes, NJ); antibodies specific for the phosphorylated state of Ser^{807}, Ser^{795}, and Ser^{807}/Thr^{811} in pRb were from New England Biolabs; anti-γ-H2AX (JBW301) was from Upstate Biotechnology (Milton Keynes, United Kingdom); anti-Ku70, anti-Ku80, and anti-α-tubulin antibodies were from Serotec (Oxford, United Kingdom).

Cell cycle and apoptosis analyses. Flow cytometric analysis was as described by Nicoletti et al. (12). Cells were analyzed on a FACScan cell scanner. Data were analyzed by the ModFit/LT (Verity Software, Topsham, ME).

In vivo *recombination assay system and analysis of homologous recombination frequency.* HeLa cells carrying a single integrated copy of a green fluorescent protein (GFP) recombination reporter construct were a gift from Prof. E. Avvedimento (Università di Napoli "Federico II," Naples, Italy). This reporter construct contains two *GFP* genes: one nonfunctional *GFP* gene mutated to contain a I-*Sce*I cleavage site and an additional, truncated *GFP* gene that can correct the *Sce*I site mutation. The I-*Sce*I restriction endonuclease is used to introduce a double-strand break (DSB) in the reporter gene. Chromosomal repair of the reporter gene by homologous recombination leads to GFP expression, which is analyzed by flow cytometry. To examine the effect of roscovitine on DSB-induced homologous recombination, HeLa cells were transiently transfected with the I-*Sce*I expression vector pCAGGS-I-*Sce*I (gift from Prof. E. Avvedimento) or with a cytomegalovirus (CMV) empty vector. Routinely, cells at ~60% confluence were transfected using LipofectAMINE reagent (Invitrogen) following the manufacturer's protocol. DNA (2 μg) per 60-mm dish was used. Roscovitine was added to the medium 6 hours after the addition of constructs. Seventy-two hours after the addition of constructs, the percentage of GFP-positive cells was determined by flow cytometry on a Becton Dickinson FACScan. To examine the effect of dominant-negative (dn) Cdk2 (dn-K2) or Cdk1 (dn-K1) on homologous recombination, HeLa-HR-GFP cells were cotransfected with the I-*Sce*I expression vector pCAGGS-I-*Sce*I and with a vector expressing either dn-K2 or dn-K1 or control empty vector (13) in a 1:1 ratio. The percentage of GFP-positive cells was determined 72 hours after the addition of constructs. To examine the effect of Cdk2, HeLa-HR-GFP cells were cotransfected with the I-*Sce*I expression vector pCAGGS-I-*Sce*I and with either a CMV control vector or the same vector expressing Cdk2 (13) in a 1:1 or 1:2 ratio. The percentage of GFP-positive cells was determined 72 hours after the addition of constructs.

Evaluation of DNA-dependent protein kinase activity. DNA-dependent protein kinase (DNA-PK) activity was estimated by using SignaTECT DNA-PK assay system (Promega, Milan, Italy) following the manufacturer's protocol. Routinely, DNA-free nuclear extracts (200-500 ng) were incubated with biotinylated peptide substrate, [γ-^{32}P]ATP, and either DNA-PK activation buffer or DNA-PK control buffer for

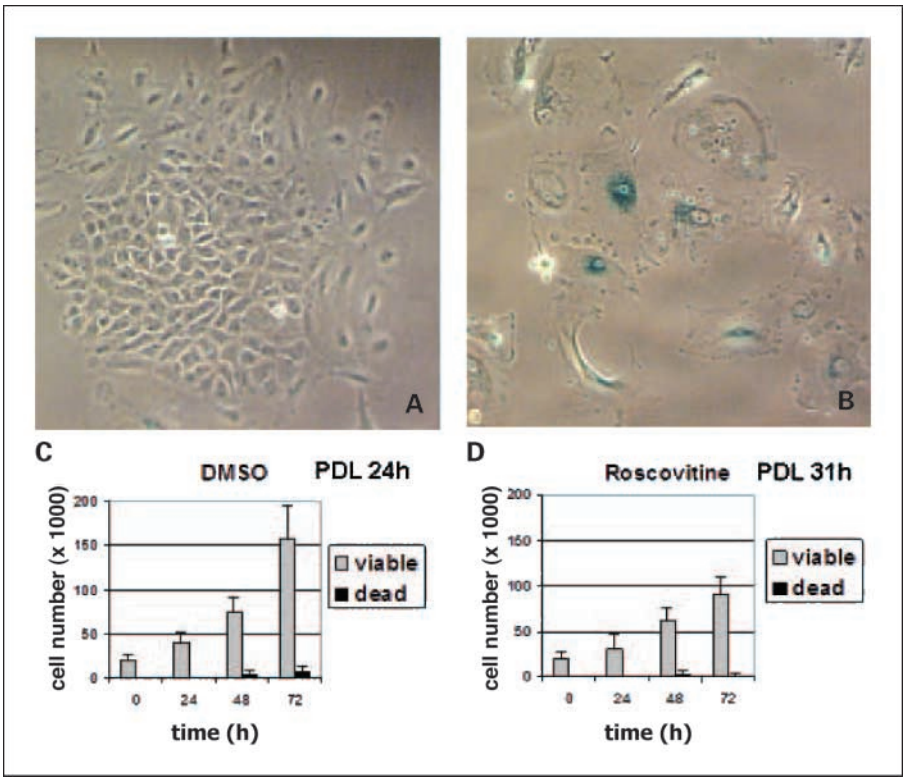

Fig. 1. Effects of doxorubicin and roscovitine in A549 cells. *A* and *B,* triplicate samples of A549 cells were incubated with doxorubicin for 48 hours. Cells were replated in drug-free medium. After 10 days, cells were stained to detect SA-β-gal activity. *A,* normal proliferating cells; *B,* morphologic alterations in senescent cells. *C* and *D,* effect of 10 μmol/L roscovitine on proliferation and viability in A549 cells. Cells were stained with trypan blue and counted at indicated times. Columns, mean cell number; bars, SE. Population doubling time (PDL) is shown for each condition.

5 minutes at 30°C. Termination buffer was added, and the reaction sample (10 μL each) was spotted onto a SAM2TM biotin capture membrane. The SAM2TM membrane squares were washed and dried before analysis by scintillation counting. The enzymatic activity of DNA-PK was calculated according to the SignaTECT protocol and normalized to the amount of Ku80 protein.

Results

Induction of premature senescence in A549 lung adenocarcinoma cell line. To investigate the ability of roscovitine to modulate drug-induced premature senescence, we first exposed the human adenocarcinoma cell line A549 to moderate doses of doxorubicin. Doxorubicin is a widely used chemotherapeutic agent believed to act primarily by stabilizing topoisomerase II-DNA complexes (14). The cellular damage is related to the accumulation of DNA DSBs. Exposure of tumor-derived cell lines to doxorubicin has been reported to induce premature senescence (4). Hence, we incubated A549 cells with 50 nmol/L doxorubicin for 48 hours, after which the cells were extensively washed and cultured in drug-free medium. After 8 days in the absence of the drug, two different types of cells were detected: normal proliferating cells, which gave rise to colonies (Fig. 1A), and cells with enlarged and flattened morphology, which stained positive for SA-β-gal (Fig. 1B). To confirm the inability of doxorubicin-induced senescent cells to proliferate, we labeled the cells with PKH2 (15). A significant fraction of highly fluorescent permanently growth-arrested cells was detected 8 days after labeling (data not shown). These data indicate that low doses of doxorubicin induce premature senescence in a substantial fraction of A549 cells.

Whereas senescence is readily induced by low doses of DNA-damaging agents, apoptosis seems to be preferentially induced at high doses. We assessed the effect of 50 nmol/L doxorubicin on apoptosis in A549 cells by flow cytometry. No observable increase in the sub-G_1 population was observed in doxorubicin-treated cells compared with controls (Fig. 2C; data not shown). In addition, analysis of molecular markers of apoptosis did not indicate induction of apoptosis (data not shown). Hence, the dose of doxorubicin selected for this study does not induce apoptosis but does induce mainly premature senescence and recovery.

Effect of roscovitine on proliferation and viability. Pharmacologic inhibitors of Cdks induce apoptosis in several tumor cell lines (8, 9). To avoid a cytotoxic effect of roscovitine in the combined treatments, we chose a concentration of the drug (10 μmol/L) that inhibits cell proliferation but does not induce cell death. As shown in Fig. 1C and D, 10 μmol/L roscovitine significantly inhibited cell proliferation, increasing doubling time from 24 to ~31 hours. However, cell viability, assessed by trypan blue exclusion assay and by flow cytometry, was not affected (Fig. 1C and D; data not shown).

Roscovitine increases doxorubicin-induced premature senescence and cell recovery after drug release. To evaluate the ability of roscovitine to modulate cellular responses to doxorubicin, A549 cells were incubated for 48 hours either with doxorubicin alone or with doxorubicin combined with roscovitine. Cells were then released and recultured in drug-free medium for 8 days. Treatment of cells with roscovitine plus doxorubicin increased the fraction of SA-β-gal-positive cells by ~30% compared with doxorubicin alone (Fig. 2A; $P < 0.001$). The effect of roscovitine on clonogenic survival was then investigated. These experiments showed a significant increase in colony formation when roscovitine was used in combination with doxorubicin (Fig. 2B; $P < 0.05$). These results show that roscovitine protects A549 cells exposed to a sublethal dose of DNA-damaging agent.

Reinforcement of G_1 arrest in doxorubicin-treated cells by roscovitine. To determine the effect of roscovitine and doxorubicin on cell cycle distribution, cells were treated either with the two drugs alone or in combination and were analyzed by flow cytometry (Fig. 2C). Roscovitine alone only slightly affected the cell cycle distribution of A549 cells. Incubation with doxorubicin resulted in accumulation of cells in G_2-M phase of the cell cycle likely due to activation of the G_2 checkpoint (16). The accumulation of cells in G_2-M was reduced in cells treated with doxorubicin plus roscovitine and was accompanied by a concomitant increase of cells in G_1 phase. Increased number of G_1 cells in combined treatment may indicate either a reinforcement of G_1 checkpoint or an abrogation of G_2 checkpoint by roscovitine. Therefore, we examined the effect of nocodazole on cell cycle distribution of treated cells. Nocodazole did not revert the effect of roscovitine (data not shown), indicating that roscovitine reinforces of G_1 checkpoint.

The ability of roscovitine to modulate G_1 cell cycle checkpoint might either depend on a direct inhibition of Cdk activity or on the modulation of cell cycle inhibitory proteins. To discriminate between these two possibilities, we examined

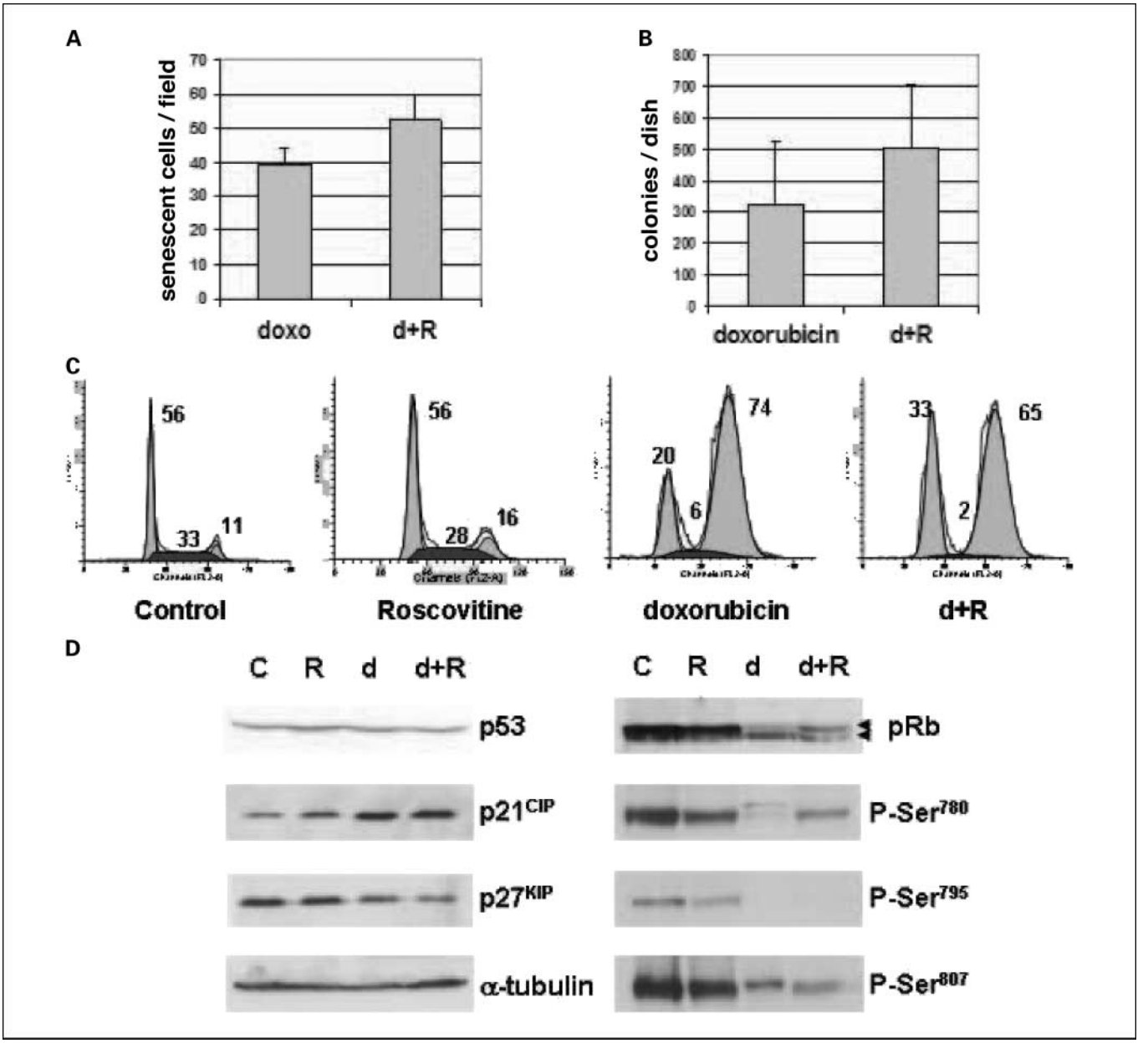

Fig. 2. Effect of combined treatment on senescence, clonogenic survival, cell cycle, and cell cycle regulators of A549 cells. *A,* triplicate samples of A549 cells were incubated either with doxorubicin (*doxo*) or with roscovitine + doxorubicin (*d+R*) for 48 hours. Cells were replated in drug-free medium. After 10 days, cells were stained to detect SA-β-gal activity. The amount of senescent cells was determined by counting of three random fields. Columns, mean of three independent experiments; bars, SE. $P < 0.001$, unpaired Student's *t* test. *B,* triplicate samples of A549 cells were incubated either with doxorubicin or with roscovitine + doxorubicin for 48 hours. Cells were replated in drug-free medium. After 8 days, colonies were stained with methylene blue. $P < 0.05$, unpaired Student's *t* test. *C,* cells were incubated with roscovitine, doxorubicin, or both for 48 hours. Numbers, percentage of cells in G_1, S, or G_2-M phase. *D,* A549 cells were incubated with roscovitine (*R*), doxorubicin (*d*), or both (*d+R*) for 48 hours and protein expression was detected by Western blot. Filters were stripped and reprobed with anti-α-tubulin antibodies as loading control.

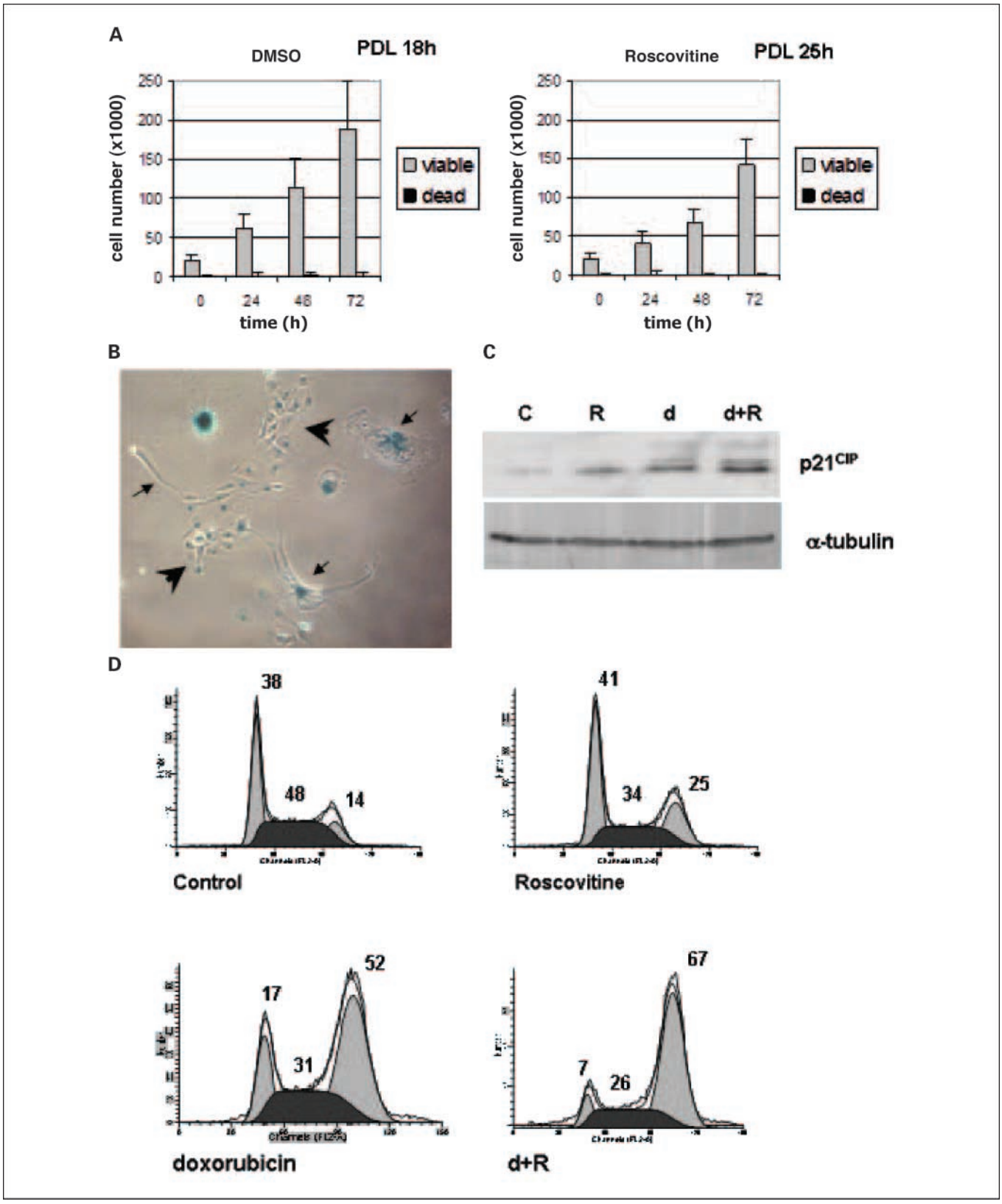

Fig. 3. Effects of doxorubicin and roscovitine in H1299 cells. *A,* effect of 10 μmol/L roscovitine on proliferation and viability in H1299 cells. Cells were stained with trypan blue and counted at indicated times. Columns, mean cell number; bars, SE. Population doubling time (PDL) is shown for each condition. *B,* morphologic alterations and SA-β-gal staining in H1299 cells. Triplicate samples of H1299 cells were incubated either with doxorubicin or with doxorubicin + roscovitine for 48 hours. Cells were replated in drug-free medium. After 10 days, cells were stained to detect SA-β-gal activity. Small arrows, morphologic alterations in senescent cells; large arrows, normal proliferating cells. *C,* $p21^{CIP}$ accumulation in doxorubicin-treated H1299 cells. Filters were stripped and reprobed with anti-α-tubulin antibodies as loading control. *D,* effect of combined treatment on cell cycle. Cells were incubated with roscovitine, doxorubicin, or both for 48 hours. Numbers, percentage of cells in G_1, S, or G_2-M phase.

the levels of cell cycle regulatory proteins. Incubation of A549 cells with the two drugs alone or in combination did not affect the level of expression of p53 as evaluated by Western blot (Fig. 2D). However, $p21^{CIP}$ was clearly induced in doxorubicin-treated cells, although no differences in $p21^{CIP}$ protein levels were detected between cells treated with doxorubicin only and cells treated with doxorubicin plus roscovitine (Fig. 2D). Protein levels of $p27^{KIP}$ were slightly reduced by doxorubicin (Fig. 2D). Consistent with the accumulation of Cdk inhibitor $p21^{CIP}$, Western blot analyses using a pan-pRb antibody showed an accumulation of the hypophosphorylated, active isoforms of the protein in cells incubated with doxorubicin and in combined treatments (Fig. 2D). Antibodies specific for the phosphorylated state of Ser^{780}, Ser^{795}, and Ser^{807}/Thr^{811} confirmed the reduced phosphorylation of pRb (Fig. 2D). These data suggest that the ability of roscovitine to reinforce G_1 checkpoint depends on direct inhibition of Cdks.

Effects of roscovitine and doxorubicin on H1299 cells. To extend the above observation to additional cell lines, we decided to investigate the effects of roscovitine in a $p53^{-/-}$ background, for which we used a lung adenocarcinoma cell line, H1299. We first evaluated the effects of low concentrations of roscovitine (10 μmol/L) on cell proliferation. As shown in Fig. 3A, 10 μmol/L roscovitine slightly inhibited proliferation of H1299 cells. In addition, viability of the cells monitored either by trypan blue exclusion method (Fig. 3A) or by fluorescence-activated cell sorting analyses (Fig. 3D) was not affected by low doses of roscovitine. Therefore, as for A549 cells, low doses of roscovitine did not activate an apoptotic response in the H1299 cell line.

We then investigated the capacity of doxorubicin to induce premature senescence in H1299 cells. H1299 cells do not express either p53 or $p16^{INK4a}$; however, it has been shown previously that inactivation of p53 and $p16^{INK4a}$ pathways does not completely abolish stress-induced senescence response in carcinoma cells (15). We exposed H1299 cells to 50 nmol/L doxorubicin for 48 hours, after which the cells were extensively washed and cultured in drug-free medium for 8 days. Morphologically altered cells, which stained positive for SA-β-gal, were easily detected in doxorubicin-treated dishes (Fig. 3B). Hence, treatment with low-dose doxorubicin induces features of premature senescence in H1299 cell line. Analysis of cell cycle regulators shows a marked accumulation of $p21^{CIP}$ in cells treated with doxorubicin (Fig. 3C). However, no differences in $p21^{CIP}$ protein levels were detected between cells treated with doxorubicin only and cells treated with

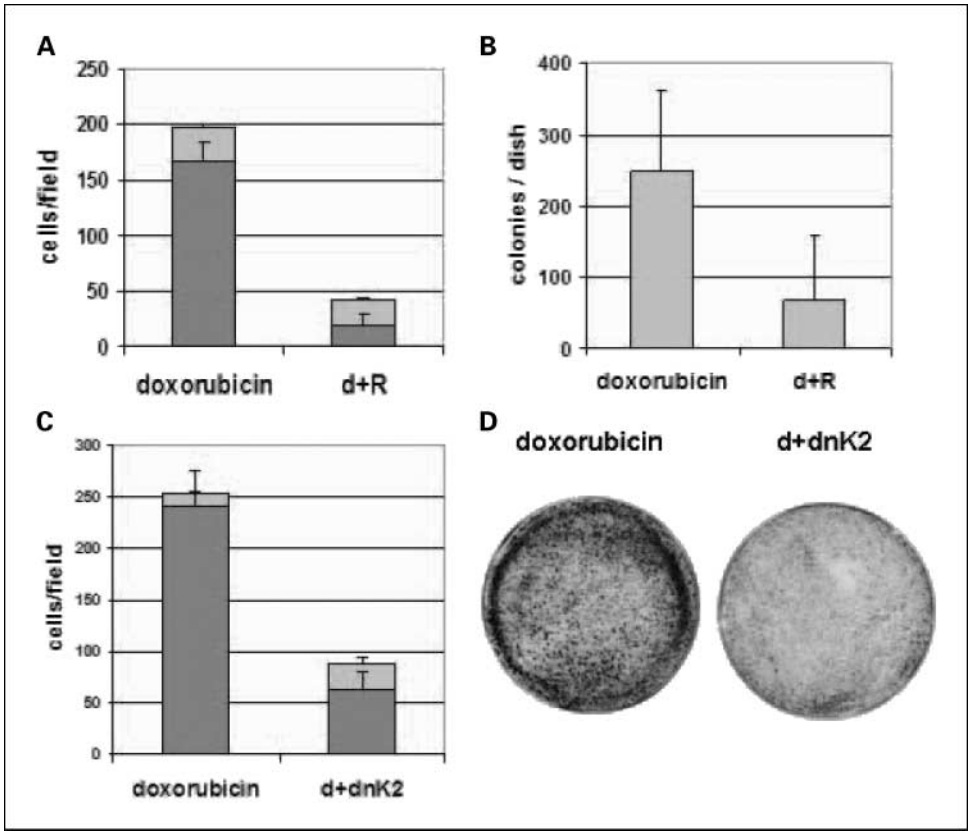

Fig. 4. Effects of roscovitine and dn-K2 in H1299 cells. *A,* effect of roscovitine on senescence. Triplicate samples of H1299 cells were incubated either with doxorubicin or with roscovitine + doxorubicin for 48 hours. Cells were replated in drug-free medium. After 10 days, cells were stained to detect SA-β-gal activity. The amount of normal (*black*) and senescent (*gray*) cells was determined by counting of three random fields. Columns, mean of three independent experiments; bars, SE. $P < 0.001$, for normal cells (unpaired Student's *t* test). *B,* effect of roscovitine on clonogenic survival. Triplicate samples of H1299 cells were incubated either with doxorubicin or with roscovitine + doxorubicin for 48 hours. Cells were replated in drug-free medium. After 8 days, colonies were stained with methylene blue. Columns, mean of three independent experiments; bars, SE. $P < 0.01$, unpaired Student's *t* test. *C,* effect of dn-K2 on senescence. Triplicate samples of H1299 cells were pretreated with doxycycline for 24 hours and subsequently incubated with doxorubicin for 48 hours. Cells were replated in drug-free medium. After 10 days, cells were stained to detect SA-β-gal activity. The amount of normal and senescent cells was determined by counting of three random fields. $P < 0.001$, for normal cells (unpaired Student's *t* test). *D,* effect of dn-K2 on clonogenic survival. Triplicate samples of H1299 cells were pretreated with doxycycline for 24 hours and subsequently incubated with doxorubicin for 48 hours. Cells were replated in drug-free medium. After 8 days, colonies were stained with methylene blue.

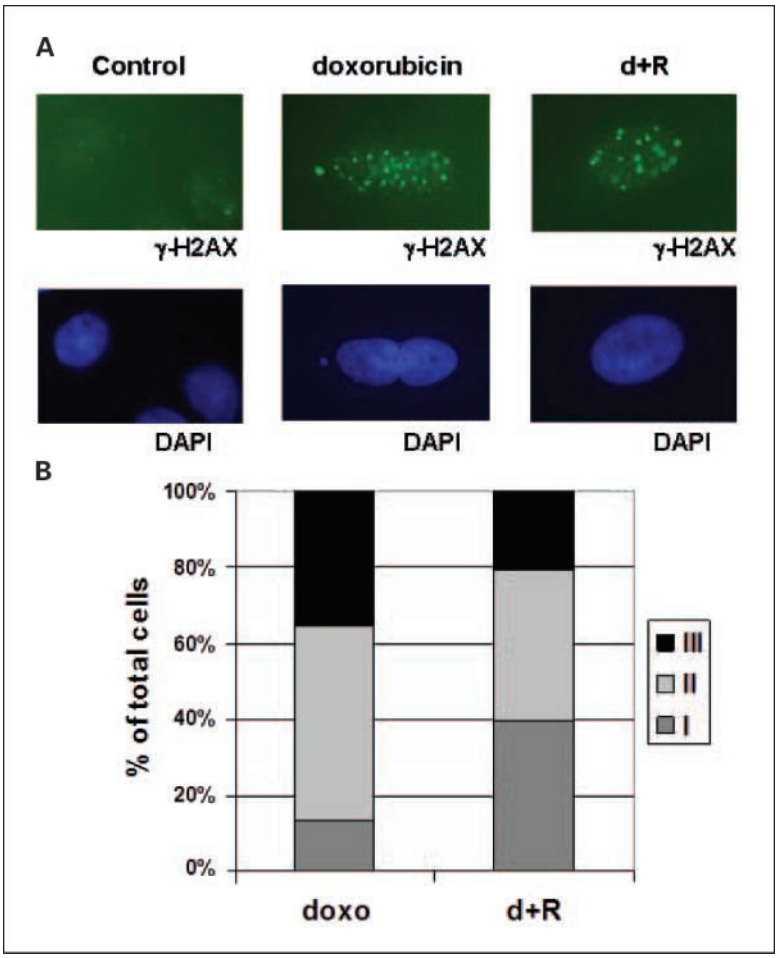

Fig. 5. Effects of roscovitine on histone H2AX phosphorylation in A549 cells. *A,* A549 cells were incubated with doxorubicin for 48 hours in the presence or absence of roscovitine. Cells were immunostained with an anti-γ-H2AX monoclonal antibody followed by secondary fluorescein conjugate antibodies. Nuclei were stained with 4′,6-diamidino-2-phenylindole (*DAPI*). *B,* frequency of foci per cell. A549 cells were incubated with doxorubicin for 48 hours in the presence or absence of roscovitine. γ-H2AX foci were counted by eye in >100 cells by capturing images of randomly chosen fields. Columns are divided into fractions of cells containing from 1 to 10 foci (class I), from 11 to 15 foci (class II), and from 16 to 20 foci (class III). $P \leq 0.01$, for class I (unpaired Student's *t* test).

doxorubicin plus roscovitine (Fig. 3C). Because neither p53 nor $p16^{INK4a}$ are expressed in H1299 cells, the observed accumulation in $p21^{CIP}$ is likely to be responsible for the induction of premature senescence following treatment with doxorubicin.

Roscovitine increases doxorubicin-dependent G_2 accumulation in H1299 cells. H1299 cells were treated with either roscovitine or doxorubicin alone or in combination for 48 hours and then analyzed by flow cytometry. As shown in Fig. 3D, treatment with low doses of roscovitine had no major effect on cell cycle distribution of asynchronously growing H1299 cells. As already observed in the A549 cell line, doxorubicin-treated cells largely accumulated in the G_2-M phase. However, unlike A549 cells, simultaneous treatment with roscovitine and doxorubicin favored the G_2-M accumulation of H1299 cells (Fig. 3D).

These results suggest that the ability of roscovitine to modulate doxorubicin-dependent checkpoints may vary in different cell lines.

Roscovitine inhibits recovery of H1299 cells after drug removal without affecting premature senescence. Roscovitine differentially affects the cell cycle distribution of doxorubicin-treated A549 and H1299 cells. To evaluate if this difference results in a different treatment outcome, H1299 cells were incubated either with doxorubicin alone or with doxorubicin plus roscovitine. Cells were then cultured in drug-free medium for 8 days and the number of normal versus senescent cells was estimated. As shown in Fig. 4A, the combination of roscovitine and doxorubicin dramatically reduced the number of normal proliferating cells ($P < 0.001$) while not affecting the number of senescent cells. Furthermore, combined treatment markedly inhibited the clonogenic survival of H1299 cells compared with doxorubicin-treated cells (Fig. 4B; $P < 0.01$).

These data show that roscovitine sensitizes H1299 cells to doxorubicin-dependent DNA damage. The differential effect observed in A549 versus H1299 cells suggests that the ability of roscovitine to reinforce the G_1 checkpoint substantially affects cell fate.

Expression of dominant-negative cyclin-dependent kinase 2 increases doxorubicin-dependent G_2 arrest and inhibits cell recovery after drug release. Pleiotropic effects of roscovitine have been reported in human tumor cell lines. Roscovitine has been shown to induce nucleolar fragmentation (17), p53 nuclear translocation (17), activation of mitogen-activated

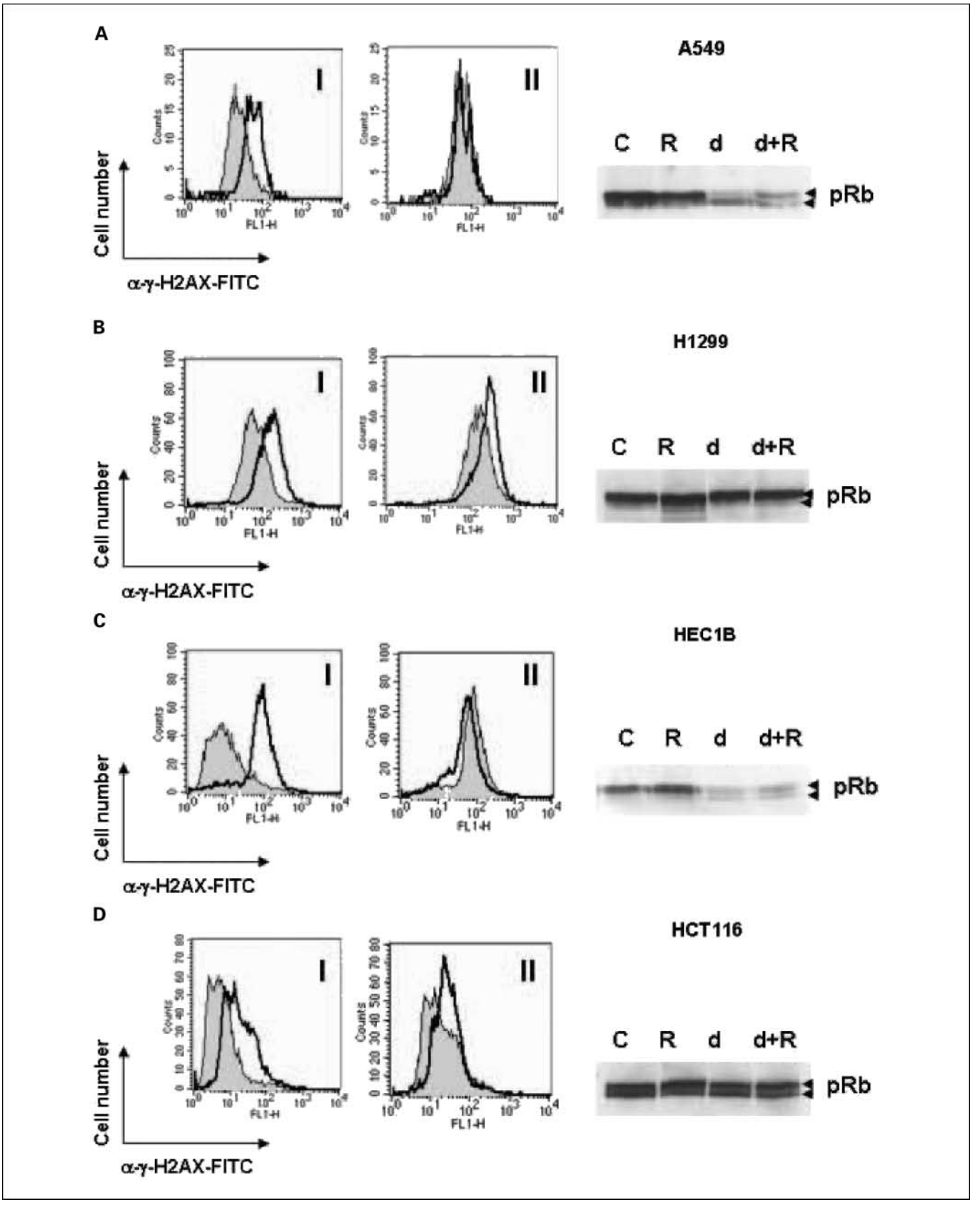

Fig. 6. Effects of roscovitine on histone H2AX phosphorylation and on pRb activation. Left, A549 (*A*), H1299 (*B*), HEC1B (*C*), and HCT116 (*D*) cells were incubated with doxorubicin for 48 hours in the presence or absence of roscovitine. Cells were immunostained with an anti-γ-H2AX monoclonal antibody followed by secondary fluorescein conjugate antibodies and analyzed by flow cytometry. I, control (*gray*) versus doxorubicin-treated cells (*bold line*); II, doxorubicin only (*gray*) versus cells treated with doxorubicin + roscovitine (*bold line*). Right, pRb phosphorylation was analyzed by Western blot using a pan-pRb antibody.

Table 1. Cell cycle distribution of adenocarcinoma cells treated with either doxorubicin alone (50 nmol/L) or with doxorubicin in combination with roscovitine (10 μmol/L) for 48 hours

Cell lines	Doxorubicin		Doxorubicin + roscovitine		p53 Status
	G_1 (%)	G_2-M (%)	G_1 (%)	G_2-M (%)	
H1299 (lung)	20	55	13	61	−/−
HCT116 (colon)	37	56	13	79	+/+
MCF-7 (breast)	65	34	45	51	+/+
HeLa (cervix)	12	83	1	86	Human papillomavirus E6
SW480 (colon)	10	72	6	82	−/−
MDA-MB-231 (breast)	2	80	1	85	−/−
A549 (lung)	20	74	32	65	+/+
HEC1B (endometrium)	3	89	17	61	ND

NOTE: ND, not determined.

protein kinase pathway (18), and inhibition of transcription (19). Because roscovitine dramatically sensitizes H1299 cells to doxorubicin, we decided to further investigate the role of Cdks in chemosensitization. We used tetracycline-inducible clones expressing a dn-K2 (13). We reported previously that overexpression of dn-K2 at high levels in H1299 cells results in G_1 cell cycle arrest and expression of several markers of premature senescence (20). Therefore, to mimic the effects of low concentrations of roscovitine, we selected three clones with very low dn-K2 expression; accordingly, induction of dn-K2 only slightly affected the cell cycle distribution of asynchronously growing H1299 cells (data not shown). Expression of dn-K2 enhanced the G_2 arrest imposed by doxorubicin in all clones (data not shown). More importantly, overexpression of dn-K2 inhibited the ability of doxorubicin-treated H1299 cells to resume proliferation (Fig. 4C; $P < 0.001$), only slightly increasing the fraction of SA-β-gal-positive cells (Fig. 4C). Clonogenic assays confirmed the ability of dn-K2 to sensitize H1299 cells to doxorubicin (Fig. 4D).

These data indicate that the chemosensitizing effect of roscovitine, observed in H1299 cells, is mediated via Cdk inhibition.

Chemoprotective and chemosensitizing effects of roscovitine correlate with the extent of DNA damage. The ability of roscovitine to reinforce the G_1 checkpoint in A549 cells is likely to be responsible for the increased resistance of the cells toward doxorubicin. To further investigate the mechanism of action of roscovitine, we examined the incidence of γ-H2AX foci in doxorubicin-treated cells. γ-H2AX is a sensitive signal for the detection of DNA DSBs (21, 22) and the number of γ-H2AX foci increases linearly with the severity of the damage (23). A549 cells were incubated either with doxorubicin alone or with doxorubicin plus roscovitine and subsequently analyzed for the presence of γ-H2AX foci by immunofluorescence microscopy. Analyses of control cells (untreated and roscovitine-treated cells) showed one or two foci in a small proportion of cells, whereas the majority of the population was negative for γ-H2AX (Fig. 5A; data not shown). Exposure of A549 cells to doxorubicin resulted in the accumulation of clearly detectable γ-H2AX foci as shown in Fig. 5A. Quantitative analysis of γ-H2AX foci distribution, in >70 nuclei, showed a significant accumulation of cells with reduced number of foci (6-10 foci per cell) in the presence of roscovitine compared with doxorubicin alone (Fig. 5B).

We next analyzed H2AX phosphorylation by flow cytometry. Flow cytometric analysis of γ-H2AX is an accurate method of measuring DNA DSBs (21) and represents a sensitive indicator of clonogenic response to chemotherapy (24). Increased intensity of fluorescence in doxorubicin-treated cells compared with controls was readily detected by flow cytometry (Fig. 6A, *left, I*). Analyses of γ-H2AX in doxorubicin versus doxorubicin plus roscovitine–treated cells confirmed the accumulation of cells with low fluorescence in the presence of roscovitine (Fig. 6A, *left, II*). These data strongly suggest a chemoprotective effect of roscovitine in A549 cells. Because roscovitine sensitizes H1299 cells to doxorubicin, combined treatment should increase the incidence of γ-H2AX foci in these cells. Indeed, combination of roscovitine and doxorubicin results in a clear shift of γ-H2AX fluorescence toward higher intensity in H1299 cells (Fig. 6B, *left, II*).

These data indicate that roscovitine modulates the extent of doxorubicin-induced DNA damage in tumor cells either increasing the susceptibility to doxorubicin (H1299 cells) or reinforcing G_1 checkpoint and survival programs (A549 cells). We decided to extend these observations to other carcinoma lines. Because the effect of roscovitine on cell survival in A549 versus H1299 correlates with the ability of roscovitine to modulate doxorubicin-dependent G_1 checkpoint, we first analyzed cell cycle distribution of a panel of carcinoma cells treated either with doxorubicin or with doxorubicin plus roscovitine. In the majority of the cell lines analyzed, roscovitine enhanced the doxorubicin-dependent G_2-M accumulation (Table 1). This effect was reproducibly detected even in cells in which doxorubicin alone induces a substantial accumulation in G_2-M (HeLa, SW480, and MDA-MB-231). Reinforcement of the G_1 checkpoint was detected in A549 and HEC1B cells (Table 1). The effect of roscovitine does not correlate with the p53 status of the cells (Table 1).

To confirm the correlation between cell cycle effect and DNA DSBs modulation, we examined γ-H2AX in HEC1B and HCT116 cells. In line with the cell cycle data, combined treatment with roscovitine and doxorubicin decreases the phosphorylation of histone H2AX in HEC1B cells (Fig. 6C, *left, II*), whereas it increases DSBs in HCT116 (Fig. 6D, *left, II*).

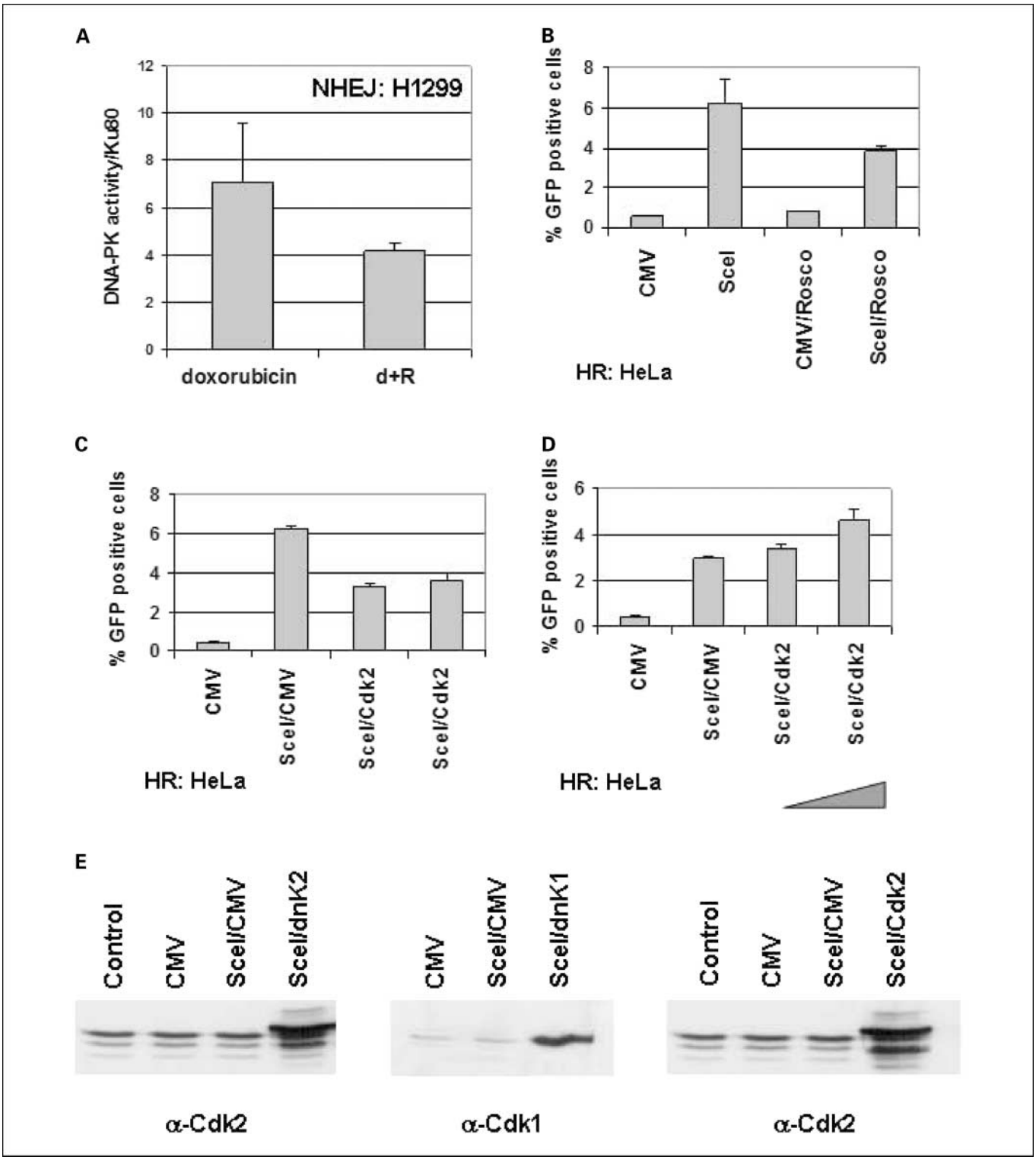

Fig. 7. Effects of roscovitine on DNA-PK activity and homologous recombination. *A,* triplicate samples of H1299 cells were incubated either with doxorubicin or with roscovitine + doxorubicin for 48 hours. DNA-PK activity was assessed on nuclear extracts and enzyme activity was normalized to Ku80 protein. Columns, mean; bars, SE; *B,* HeLa cells were transiently transfected with either control vector (CMV) or I-*Sce*I endonuclease in the absence or presence of 10 μmol/L roscovitine (*Rosco*). The efficiency of homologous recombination was estimated by flow cytometry. Columns, mean of three independent experiments; bars, SE. $P \leq 0.01$, unpaired Student's *t* test. *C,* HeLa cells were transiently cotransfected with I-*Sce*I endonuclease together with either dnK2 or dnK1 or empty control vector (*CMV*). The efficiency of homologous recombination was estimated by flow cytometry. Columns, mean of three independent experiments; bars, SE. $P < 0.001$, for dnK2; $P = 0.001$, for dnK1 (unpaired Student's *t* test). *D,* HeLa cells were transiently cotransfected with I-*Sce*I endonuclease together with either empty control vector or Cdk2 in a 1:1 or 1:2 ratio. The efficiency of homologous recombination was estimated by flow cytometry. Columns, mean of three independent experiments; bars, SE. $P \leq 0.01$, unpaired Student's *t* test. *E,* HeLa cells were transiently cotransfected with I-*Sce*I endonuclease together with either empty control vector or dnK2 or dnK1 or Cdk2. Untransfected cells were used as control. Expression of transfected proteins was assessed by Western blot using anti-Cdk2 and anti-Cdc2 antibodies.

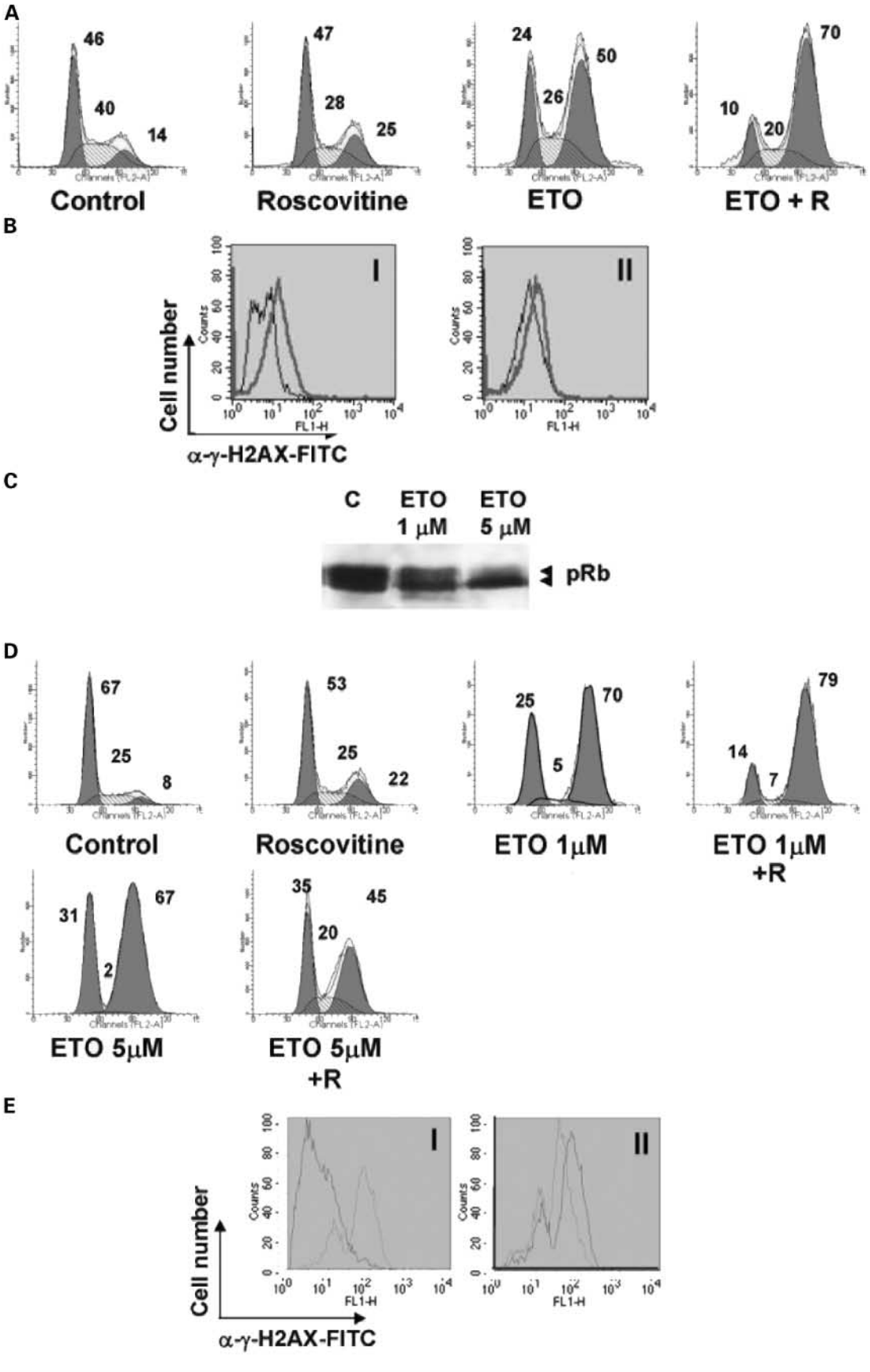
A
46
40
14
Control
47
28
25
Roscovitine
24
26
50
ETO
10
20
70
ETO + R
B
I
II
Cell number
Counts
FL1-H
α-γ-H2AX-FITC
C
C
ETO 1 μM
ETO 5 μM
pRb
D
67
25
8
Control
53
25
22
Roscovitine
25
5
70
ETO 1μM
14
7
79
ETO 1μM +R
31
2
67
ETO 5μM
35
20
45
ETO 5μM +R
E
I
II
Cell number
Counts
FL1-H
α-γ-H2AX-FITC

These findings show a general ability of roscovitine to modulate the extent of doxorubicin-induced DNA damage in tumor cells, which ultimately affects the outcome of treatment. However, roscovitine seems to either synergize or antagonize with doxorubicin in different cells. Because pRb plays a key role in G_1 checkpoint (25) and is also required for intra-S response to DNA damage (26, 27), we analyzed pRb phosphorylation status in A549, HEC1B, H1299, and HCT116 cells. An accumulation of hypophosphorylated, active pRb was readily detected in A549 and HEC1B cells incubated with doxorubicin (Fig. 6A and C, *right*). In contrast, no variation in pRb phosphorylation pattern was observed in both H1299 and HCT116 after treatment with doxorubicin (Fig. 6B and D, *right*). These data suggest that the ability of roscovitine to reinforce doxorubicin-dependent G_1 checkpoint may require active pRb.

Roscovitine modulates DNA repair pathways in doxorubicin-treated cells. The results described indicate that roscovitine can sensitize certain tumor cells to doxorubicin, increasing the amount of DNA DSBs. There are two main pathways for DNA DSBs repair: homologous recombination and nonhomologous end-joining (NHEJ; ref. 28), which cooperate *in vivo* (29). In a previous study (30), the ability of roscovitine to negatively modulate NHEJ pathway in cells treated with ionizing radiation has been reported. Therefore, we analyzed the activity of DNA-PK in H1299 cells treated either with doxorubicin alone or with doxorubicin plus roscovitine. We found that roscovitine decreases DNA-PK activity in doxorubicin-treated H1299 by ~40% (Fig. 7A). Western blot analyses confirmed (30) that roscovitine affect neither Ku70 nor Ku80 protein levels (data not shown). These results confirm that roscovitine negatively modulates DNA-PK activity and inhibits NHEJ repair pathway in H1299 cells.

In mammalian cells, the NHEJ pathway predominates during G_0 and G_1 phases, whereas homologous recombination is preferentially active in S and G_2 phases (31, 32). Because the chemosensitizing effect of roscovitine enhanced G_2-M accumulation, we decided to evaluate whether the homologous recombination repair pathway was affected by roscovitine using an *in vivo* recombination assay system.

We used a HeLa cell line that carries an integrated copy of a GFP recombination reporter construct. The I-*Sce*I restriction endonuclease is used to introduce a DSB in the reporter gene. Repair of the reporter gene by homologous recombination leads to GFP expression, which is quantitatively analyzed by flow cytometry.

We transiently transfected HeLa cells with I-*Sce*I endonuclease or with a control, empty vector, in the absence or presence of 10 μmol/L roscovitine and determined the efficiency of homologous recombination by flow cytometry. As shown in Fig. 7B, 10 μmol/L roscovitine reduced the efficiency of recombinational repair by ~30% ($P \leq 0.01$). No effects of roscovitine on transfection efficiency of control plasmids in HeLa cells were observed (data not shown). To further substantiate a role for Cdks in modulation of homologous recombination repair, HeLa cells were transiently cotransfected with I-*Sce*I endonuclease together with either dn-K2 or dn-K1 (13) or empty vector. Flow cytometric analyses show that transient expression of dn-K2 inhibited recombinational repair by ~50% (Fig. 7C; $P < 0.001$), whereas dn-K1 inhibited repair by ~40% (Fig. 7C; $P = 0.001$). Furthermore, cotransfection of I-*Sce*I endonuclease with increasing amounts of Cdk2 resulted in a dose-dependent increase in homologous recombination repair (Fig. 7D; $P \leq 0.01$). Expression of transfected proteins was assessed by Western blot (Fig. 7E). These results indicate that inhibition of Cdk2 and Cdk1 activity, either by pharmacologic agent or by dominant-negative isoforms, results in decreased homologous recombination repair.

These experiments show that roscovitine affects DNA repair processes in tumor cells, which results in tumor chemosensitization.

Effects of roscovitine and etoposide on H1299 cells. To extend the above observations to other topoisomerase II inhibitors, H1299 cells were treated with either roscovitine or etoposide alone or in combination for 48 hours and then analyzed by flow cytometry. As shown in Fig. 8A, etoposide-treated cells largely accumulated in the G_2-M phase. Simultaneous treatment with roscovitine and etoposide favored the G_2-M accumulation of H1299 cells (Fig. 8A). To confirm the correlation between cell cycle effect and DNA DSBs modulation, we examined H2AX phosphorylation. In line with the cell cycle data, combined treatment with roscovitine and etoposide increased DSBs in H1299 cells (Fig. 8B, *left, II*). These data indicate that roscovitine also modulates the extent of etoposide-induced DNA damage in H1299 cells.

Reinforcement of pRb-dependent G_1 arrest in etoposide-treated A549 cells by roscovitine. We next investigated the ability of roscovitine to modulate etoposide-dependent G_1 checkpoint in A549 cells. Because etoposide is not as effective as doxorubicin in inducing a G_1 arrest response (33), we first evaluated the effect of different sublethal concentrations of etoposide on pRb activation. Treatment of A549 cells with 1 μmol/L etoposide only induced partial dephosphorylation in pRb protein, whereas a higher concentration (5 μmol/L) was effective in activating pRb (Fig. 8C; data not shown). Both concentrations resulted in accumulation of A549 cells in G_2-M phase (Fig. 8D). Next, we assessed the ability of roscovitine to reinforce the G_1 checkpoint in etoposide-treated A549 cells. Interestingly, whereas roscovitine effectively reinforced the G_1 arrest in cells treated with the higher concentration of etoposide (Fig. 8D), simultaneous treatment with 1 μmol/L etoposide and roscovitine favored the G_2-M accumulation (Fig. 8D). These data

Fig. 8. Effects of etoposide and roscovitine in H1299 and in A549 cells. *A,* H1299 cells were incubated with roscovitine (10 μmol/L), etoposide (1 μmol/L), or both for 48 hours. Numbers, percentage of cells in G_1, S, or G_2-M phase. The percentage of apoptotic, sub-G_1 cells, estimated by flow cytometric analyses, never exceeded 5% in all conditions studied. *B,* H1299 cells were incubated with 1 μmol/L etoposide for 48 hours in the presence or absence of roscovitine. Cells were immunostained with an anti-γ-H2AX monoclonal antibody followed by secondary fluorescein conjugate antibodies and analyzed by flow cytometry. I, control (*black line*) versus etoposide-treated cells (*red line*); II, etoposide only (*black line*) versus cells treated with etoposide + roscovitine (*red line*). *C,* pRb phosphorylation status in A549 cells was analyzed by Western blot using a pan-pRb antibody. *D,* A549 cells were incubated with roscovitine, etoposide, or both for 48 hours. Numbers, percentage of cells in G_1, S, or G_2-M phase. The percentage of apoptotic, sub-G_1 cells, estimated by flow cytometric analyses, never exceeded 5% in all conditions studied. *E,* A549 cells were incubated with 5 μmol/L etoposide for 48 hours in the presence or absence of roscovitine. Cells were immunostained with an anti-γ-H2AX monoclonal antibody followed by secondary fluorescein conjugate antibodies and analyzed by flow cytometry. I, control (*black line*) versus etoposide-treated cells (*red line*); II, etoposide only (*black line*) versus cells treated with etoposide + roscovitine (*red line*).

further suggest that the ability of roscovitine to reinforce DNA damage–dependent G_1 checkpoint may require active pRb. Finally, we examined the effect of increased G_1 arrest on the incidence of γ-H2AX foci in etoposide-treated A549 cells. Combination of roscovitine and 5 μmol/L etoposide substantially decreased DSBs in A549 cells (Fig. 8E, *left, II*). In contrast, roscovitine did not change H2AX phosphorylation in cells treated with 1 μmol/L etoposide (data not shown). These data further suggest that the chemoprotective effect of roscovitine in A549 cells requires pRb activation.

Discussion

Because inhibition of Cdk activity seems to be a major event in cellular responses to sublethal DNA damage, we investigated the effects of roscovitine, a pharmacologic inhibitor of Cdk activity, on doxorubicin-induced senescence in human carcinoma cells. Our results show that treatment of A549 lung adenocarcinoma cells with sublethal doses of doxorubicin induces senescence in a substantial fraction of the cells. Roscovitine significantly potentiates this response, increasing the fraction of SA-β-gal-positive cells by ~30%. In addition, a consistent increase in clonogenic survival was detected when cells were treated with roscovitine and doxorubicin compared with doxorubicin alone. These data together indicate a chemoprotective effect of roscovitine in A549 cells. Similar results were obtained in HEC1B cells.

The protective effect of roscovitine is correlated to a cell cycle inhibitory function, which results in an increased cell cycle block at G_1 phase. G_1 cell cycle arrest has been correlated previously with decreased susceptibility to chemotherapeutic drugs (34, 35). In addition, expression of $p21^{CIP}$ and $p16^{INK4}$ (which results in G_1 arrest) was reported to negatively regulate apoptosis (5, 36). Up-regulation of $p21^{CIP}$ has also been associated with drug resistance (37) and $p21^{CIP}$ has been shown to play a key role in G_1 checkpoint maintenance (25). pRb represents a key target for Cdk inhibitors in G_1 checkpoint. In addition, recent data show a critical role for pRb in DNA damage–dependent intra-S checkpoint (26, 27). Consistent with the up-regulation of $p21^{CIP}$, hypophosphorylated, active isoforms of pRb accumulate in both A549 and HEC1B cells treated with doxorubicin. Analyses of cell cycle regulators in these cells suggest that roscovitine reinforces the G_1 checkpoint by direct inhibition of Cdk2 and Cdk1. Hence, roscovitine seems to synergize with a $p21^{CIP}$-dependent, pRb-mediated G_1 cell cycle arrest.

The augmentation of G_1 arrest correlated with the extent of DNA damage: roscovitine reduces the amount of γ-H2AX foci in A549 and HEC1B cells. The negative correlation between G_1 arrest and DNA damage is further supported by analyses of other cell lines. In fact, lack of G_1 arrest and augmentation of G_2-M accumulation in other cells correlates with an increase in DNA DSBs. By lowering the level of doxorubicin-induced DNA damage roscovitine may easily facilitate both premature senescence and repair programs in A549 and HEC1B cells, thus inducing chemoprotection.

Analyses of H1299 cells highlighted an unexpected ability of roscovitine to potentiate both doxorubicin and etoposide cytotoxicity. Our data show that a nontoxic concentration of roscovitine, with minimal effects on cell proliferation, renders H1299 cells significantly more susceptible to doxorubicin. In these cells, roscovitine does not modulate senescence but markedly reduces the capacity of cells to repair damage and to resume proliferation after treatment. As discussed above, this sensitizing effect of roscovitine correlates with an increased accumulation of cells in G_2-M. This potentiation of G_2-M blockade is likely secondary to increased DNA damage. Augmentation of DSBs in roscovitine plus doxorubicin–treated cells would lead to enhanced G_2-M checkpoint activation and to G_2-M-phase cell accumulation. These unexpected findings were extended to several other carcinoma cells in which combined treatment with roscovitine and doxorubicin, or etoposide, was found to enhance G_2-M accumulation, to increase the amount of γ-H2AX foci, and to inhibit DNA repair.

Two main repair pathways, homologous recombination and NHEJ, cooperate to repair DNA DSBs (28). We investigated the ability of roscovitine to modulate these two processes in doxorubicin-treated cells. We first confirmed the ability of roscovitine to negatively modulate DNA-PK activity in H1299 cells (30). Then, we investigated the effect of roscovitine on homologous recombination repair. Our data show that roscovitine significantly reduces the efficiency of recombinational repair and identify a novel mechanism of action by which roscovitine affects tumor cells: inhibition of DNA DSBs repair. Pleiotropic effects of roscovitine have been reported in human tumor cell lines (17–19), which prompted us to further substantiate the role of Cdk2 and Cdk1 kinases as targets of roscovitine in tumor chemosensitization. Experiments with inducible dn-K2 clones indicate that loss of Cdk2 and Cdk1 activity is indeed responsible for the chemosensitizing effect of roscovitine. Overexpression of dn-K2 in H1299 cells, in fact, potentiated doxorubicin-induced G_2-M arrest and inhibited recovery of the cells after treatment (Fig. 4). It is worth noting that overexpression of dn-K2 results in both Cdk2 and Cdk1 inhibition (13). Furthermore, analyses of homologous recombination in HeLa cells transiently overexpressing either dn-K2 or dn-K1 or Cdk2 confirmed a role for Cdks in modulation of DNA repair processes (Fig. 7). Recently, a role for Cdk in the control of DNA repair pathways has been shown in yeast cells (38, 39).

These data support a therapeutic potential for roscovitine combined with doxorubicin in tumor treatment. An ability of various pharmacologic Cdk inhibitors to enhance cytotoxicity has been noted in other tumor cell systems and has been correlated to lack of functional p53 protein (30, 34). In contrast, the chemosensitizing effect that we report involves both $p53^{-/-}$ (H1299, HeLa, SW480, and MDA-MB-231) and $p53^{+/+}$ (HCT116 and MCF-7) cell lines. However, it is worth noting that the doses of doxorubicin used in this study are sublethal and almost exclusively activate senescence and repair pathways. Therefore, combined treatment with roscovitine and doxorubicin in our system seems to increase a nonapoptotic, delayed death response likely due to mitotic catastrophe. Hence, combined treatment of roscovitine and DNA-damaging agents not only enhances drug-induced apoptosis (40, 41) but also effectively hampers the recovery of mildly damaged tumor cells after treatment.

In conclusion, the results described above indicate that roscovitine, by hindering both homologous recombination and NHEJ repair processes, has the potential to inhibit recovery of mildly damaged tumor cells after doxorubicin

treatment and to increase the susceptibility of tumor cells to chemotherapy.

However, analyses of A549 and HEC1B cells suggests that in some tumor cell lines the cell cycle inhibitory function of roscovitine prevails on the DNA repair inhibitory activity. In these settings, roscovitine can reinforce DNA damage–dependent G_1 checkpoint, favoring survival programs. This raises the possibility that treatment with roscovitine might promote resistance to chemotherapeutic drugs in some tumors.

To investigate possible mechanisms for the differential effects of roscovitine, we evaluated pRb phosphorylation status in A549, HEC1B, H1299, and HCT116 cells. In line with its central role in G_1 cell cycle checkpoint, activation of pRb became readily apparent in both A549 and HEC1B cells after incubation with doxorubicin (or etoposide). Surprisingly, H1299 and HCT116 cells, treated in the same way, did not show any significant accumulation of hypophosphorylated pRb, suggesting that DNA damage–dependent activation of pRb in these cells is compromised. pRb activation defect in tumor cell lines has been reported previously (42). These data suggest that the ability of roscovitine to reinforce the doxorubicin-dependent (or etoposide-dependent) G_1 checkpoint might require the presence of active pRb. This work represents a novel mechanism for combined chemotherapy that may have widespread application to treating carcinomas.

Acknowledgments

We thank Prof. E. Avvedimento for generous gift of recombination assay system and Dr. Mike Hubank (University College London) for helpful advice.

References

1. Roninson IB, Brode EV, Chang BD. If not apoptosis, then what? Treatment-induced senescence and mitotic catastrophe in tumor cells. Drug Resist Updat 2001;4:303–13.
2. Johnstone RW, Ruefli AA, Lowe SW. Apoptosis: a link between cancer genetics and chemotherapy. Cell 2002;108:153–64.
3. te Poele RH, Okorokov AL, Jardine L, Cummings J, Joel SP. DNA damage is able to induce senescence in tumor cells *in vitro* and *in vivo*. Cancer Res 2002;62:1876–83.
4. Chang BD, Broude EV, Dokmanovic M, et al. A senescence-like phenotype distinguishes tumor cells that undergo terminal proliferation arrest after exposure to anticancer agents. Cancer Res 1999;59:3761–7.
5. Schmitt CA, Fridman JS, Yang M, et al. A senescence program controlled by p53 and $p16^{INK4a}$ contributes to the outcome of cancer therapy. Cell 2002;109:335–46.
6. Zhou BB, Bartek J. Targeting the checkpoint kinases: chemosensitization versus chemoprotection. Nat Rev Cancer 2004;4:216–25.
7. Meijer L, Borgne A, Mulner O, et al. Biochemical and cellular effects of roscovitine, a potent and selective inhibitor of the cyclin-dependent kinases cdc2, cdk2 and cdk5. Eur J Biochem 1997;243:527–36.
8. Mgbonyebi OP, Russo J, Russo IH. Roscovitine induces cell death and morphological changes indicative of apoptosis in MDA-MB-231 breast cancer cells. Cancer Res 1999;59:1903–10.
9. Hahntow IN, Schneller F, Oelsner M, et al. Cyclin-dependent kinase inhibitor roscovitine induces apoptosis in chronic lymphocytic leukemia cells. Leukemia 2004;18:747–55.
10. Dimri GP, Lee X, Basile G, et al. A biomarker that identifies senescent human cells in culture and in aging skin *in vivo*. Proc Natl Acad Sci U S A 1995;92:9363–7.
11. Laemmli UK. Cleavage of structural proteins during the assembly of the head of bacteriophage T4. Nature 1970;227:680–5.
12. Nicoletti I, Migliorati G, Pagliacci MC, Grignani F, Riccardi C. A rapid and simple method for measuring thymocyte apoptosis by propidium iodide staining and flow cytometry. J Immunol Methods 1991;139:271–9.
13. Hu B, Mitra J, van den Heuvel S, Enders GH. S and G_2 phase roles for Cdk2 revealed by inducible expression of a dominant-negative mutant in human cells. Mol Cell Biol 2001;21:2755–66.
14. Liu LF. DNA topoisomerase poisons as antitumor drugs. Annu Rev Biochem 1989;58:351–75.
15. Chang BD, Swift ME, Shen M, Fang J, Broude EV, Roninson IB. Molecular determinants of terminal growth arrest induced in tumor cells by a chemotherapeutic agent. Proc Natl Acad Sci U S A 2002;99:389–94.
16. Xiao Z, Chen Z, Gunasekera AH, et al. Chk1 Mediates S and G_2 arrests through Cdc25A degradation in response to DNA-damaging agents. J Biol Chem 2003;278:21767–73.
17. David-Pfeuty T. Potent inhibitors of cyclin-dependent kinase 2 induce nuclear accumulation of wild-type p53 and nucleolar fragmentation in human untransformed and tumor-derived cells. Oncogene 1999;18:409–22.
18. Whittaker SR, Walton MI, Garrett MD, Workman P. The cyclin-dependent kinase inhibitor CYC202 (*R*-roscovitine) inhibits retinoblastoma protein phosphorylation, causes loss of cyclin D1, and activates the mitogen-activated protein kinase pathway. Cancer Res 2004;64:262–72.
19. Hajduch M, Havlieek L, Vesely J, Novotny R, Mihal V, Strnad M. Synthetic cyclin dependent kinase inhibitors. New generation of potent anti-cancer drugs. Adv Exp Med Biol 1999;457:341–53.
20. Crescenzi E, Palumbo G, Brady HJ. Bcl-2 activates a programme of premature senescence in human carcinoma cells. Biochem J 2003;375:263–74.
21. Rogakou EP, Pilch DR, Orr AH, Ivanova VS, Bonner WM. DNA double-stranded breaks induce histone H2AX phosphorylation on serine 139. J Biol Chem 1998;273:5858–68.
22. Sedelnikova OA, Rogakou EP, Panyutin IG, Bonner WM. Quantitative detection of (125)IdU-induced DNA double-strand breaks with γ-H2AX antibody. Radiat Res 2002;158:486–92.
23. Olive PL, Banath JP. Phosphorylation of histone H2AX as a measure of radiosensitivity. Int J Radiat Oncol Biol Phys 2004;58:331–5.
24. Banath JP, Olive PL. Expression of phosphorylated histone H2AX as a surrogate of cell killing by drugs that create DNA double-strand breaks. Cancer Res 2003;63:4347–50.
25. Bartek J, Lukas J. Mammalian G_1- and S-phase checkpoints in response to DNA damage. Curr Opin Cell Biol 2001;13:738–47.
26. Knudsen KE, Booth D, Naderi S, et al. RB-dependent S-phase response to DNA damage. Mol Cell Biol 2000;20:7751–63.
27. Bosco EE, Mayhew CN, Hennigan RF, Sage J, Jacks T, Knudsen ES. RB signaling prevents replication-dependent DNA double-strand breaks following genotoxic insult. Nucleic Acids Res 2004;32:25–34.
28. Jackson SP. Sensing and repairing DNA double-strand breaks. Carcinogenesis 2002;23:687–96.
29. Couedel C, Mills KD, Barchi M, et al. Collaboration of homologous recombination and nonhomologous end-joining factors for the survival and integrity of mice and cells. Genes Dev 2004;18:1293–304.
30. Maggiorella L, Deutsch E, Frascogna V, et al. Enhancement of radiation response by roscovitine in human breast carcinoma *in vitro* and *in vivo*. Cancer Res 2003;63:2513–7.
31. Johnson RD, Jasin M. Sister chromatid gene conversion is a prominent double-strand break repair pathway in mammalian cells. EMBO J 2000;19:3398–407.
32. Rothkamm K, Kruger I, Thompson LH, Lobrich M. Pathways of DNA double-strand break repair during the mammalian cell cycle. Mol Cell Biol 2003;23:5706–15.
33. Attardi LD, de Vries A, Jacks T. Activation of the p53-dependent G_1 checkpoint response in mouse embryo fibroblasts depends on the specific DNA damage inducer. Oncogene 2004;23:973–80.
34. Sugiyama K, Shimizu M, Akiyama T, et al. UCN-01 selectively enhances mitomycin C cytotoxicity in p53 defective cells which is mediated through S and/or G(2) checkpoint abrogation. Int J Cancer 2000;85:703–9.
35. Stewart ZA, Mays D, Pietenpol JA. Defective G_1-S cell cycle checkpoint function sensitizes cells to microtubule inhibitor-induced apoptosis. Cancer Res 1999;59:3831–7.
36. Lu Y, Tatsuka M, Takebe H, Yagi T. Involvement of cyclin-dependent kinases in doxorubicin-induced apoptosis in human tumor cells. Mol Carcinog 2000;29:1–7.
37. Zhang W, Kornblau SM, Kobayashi T, Gambel A, Claxton D, Deisseroth AB. High levels of constitutive WAF1/Cip1 protein are associated with chemoresistance in acute myelogenous leukemia. Clin Cancer Res 1995;1:1051–7.
38. Ira G, Pellicioli A, Balijja A, et al. DNA end resection, homologous recombination and DNA damage checkpoint activation require CDK1. Nature 2004;431:1011–7.
39. Aylon Y, Liefshitz B, Kupiec M. The CDK regulates repair of double-strand breaks by homologous recombination during the cell cycle. EMBO J 2004;23:4868–75.
40. Lu W, Chen L, Peng Y, Chen J. Activation of p53 by roscovitine-mediated suppression of MDM2 expression. Oncogene 2001;20:3206–16.
41. Blaydes JP, Craig AL, Wallace M, et al. Synergistic activation of p53-dependent transcription by two cooperating damage recognition pathways. Oncogene 2000;19:3829–39.
42. Broceno C, Wilkie S, Mittnacht S. RB activation defect in tumor cell lines. Proc Natl Acad Sci U S A 2002;99:14200–5.